

## Electron Microscopic Studies of Modulated Structures in $(\text{Au},\text{Ag})\text{Te}_2$

### III. Krennerite

G. VAN TENDELOO AND S. AMELINCKX\*

*Rijksuniversitair Centrum Antwerpen, B-2020 Antwerpen, Belgium*

AND P. GREGORIADES

*University of Thessaloniki, Thessaloniki, Greece*

Received October 19, 1983; in revised form January 16, 1984

The structure of krennerite ( $\text{Au}_{0.8}\text{Ag}_{0.2}\text{Te}_2$ ) as determined using X-ray diffraction, is confirmed by means of electron diffraction and high resolution electron microscopy. The structure can be considered as a twin interface modulated long period superstructure of calaverite. The images suggest that gold and silver are ordered, silver being preferentially located along the twin interface. Planar defects associated with variable width of the twin lamellae are discussed in detail and a structural model can be deduced from the high resolution observations.

#### 1. Introduction

In parts I and II of this paper (1, 2) we reported on electron microscopic studies, respectively, of gold telluride  $\text{AuTe}_2$  (calaverite) and on the mixed telluride  $\text{AuAgTe}_2$  (sylvanite). It was shown that both compounds exhibit deformation modulated structures with approximately the same long period. The modulation period is incommensurate in calaverite and in nonstoichiometric sylvanite; it is commensurate in stoichiometric sylvanite. Moreover, off-stoichiometric sylvanite was found to exhibit also a long period antiphase boundary modulation with the same period as the deformation modulated structure.

Here in part III we report on a third compound of the same series, krennerite, with a normal composition in the neighborhood of  $\text{Ag}_{0.2}\text{Au}_{0.8}\text{Te}_2$ .

\* Also at SCK/CEN, B-2400 Mol, Belgium.

#### 2. Materials and Specimen Preparation

The material was prepared by melting the constituent elements in the required proportions in an evacuated quartz capsule, followed by slow cooling, in the same manner as the other compounds in this series (1, 2). The materials are brittle and specimens for electron microscopy were obtained by crushing fragments of the ingots. The material cleaves preferentially along the *c*-plane and specimens are therefore mostly oriented with this plane parallel with the plane of the grid.

#### 3. The Crystal Structure

The crystal structure was determined by Tunell and Pauling, using X-ray diffraction (3); it is closely related to that of calaverite. The symmetry is orthorhombic, the space group being *Pma* and the lattice parameters  $a = 1.654$  nm;  $b = 0.882$  nm;  $c =$

0.446 nm. The base vectors of the lattice are related to those of calaverite by means of the relation

$$\begin{pmatrix} a \\ b \\ c \end{pmatrix}_{\text{krennerite}} = \begin{pmatrix} \frac{4}{3} & 0 & \frac{5}{3} \\ -1 & 0 & 1 \\ 0 & 0 & 1 \end{pmatrix} \begin{pmatrix} a \\ b \\ c \end{pmatrix}_{\text{calaverite}}$$

A projection on the  $c$ -plane is represented in Fig. 1a. When compared with the  $b$ -projection of calaverite (1) it becomes evident that krennerite can be derived from calaverite by subunit cell twinning. The pseudocubic lattice (see (1)) which is viewed along the  $[110]_{\text{cub}}$  direction in this projection, is continuous across the twin boundary. The two twin related lamella can be regarded as two orientation variants of the calaverite structure, built on the same quasicubic basic lattice. The sideview of the structure along the  $b$ -axis (Fig. 1b) is very similar to that of calaverite.

From X-ray diffraction there is no evidence for the ordering of gold and silver.

The krennerite structure can in fact be considered as a commensurate, interface modulated structure the twin planes being parallel with the planes of constant phase in calaverite and with the antiphase boundary planes in sylvanite.

#### 4. Reciprocal Lattice and Diffraction Patterns

The most relevant diffraction pattern is that along the  $[001]$  zone, along which the structure of Fig. 1a was projected. A representative pattern is reproduced in Fig. 2a; the long period is clearly visible; it is equal to eight times the projected pseudocubic period, the first pseudocubic spot being indexed 800 in the krennerite lattice. The distance between the (202) spot and the origin is now divided in eight intervals by superstructure spots in such a way that  $(202)_{\text{cal}}$  coincides with  $(800)_{\text{Kr}}$ . Also the pseudo-hexagonal zone  $[01\bar{3}]$  prominently exhibits the

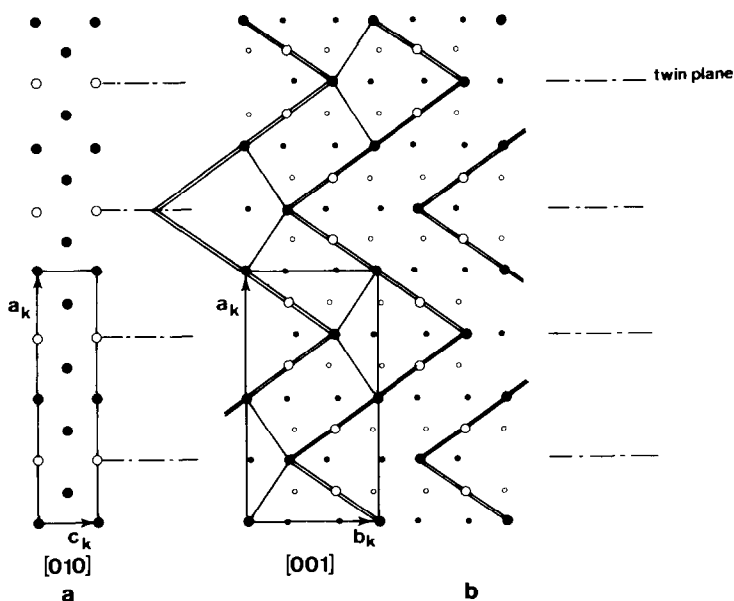


FIG. 1. Crystal structure of krennerite ( $\text{Au}_{0.8}\text{Ag}_{0.2}\text{Te}_2$ ) as projected along the  $[001]$  and  $[010]$  directions. (a) In the  $[010]$  zone all atom columns have the composition  $(\text{Au}, \text{Ag})\text{Te}_2$ . (b) In the  $[001]$  zone the large circles represent either gold or silver columns, the small ones are tellurium columns; the dash-dot lines are twin interfaces.

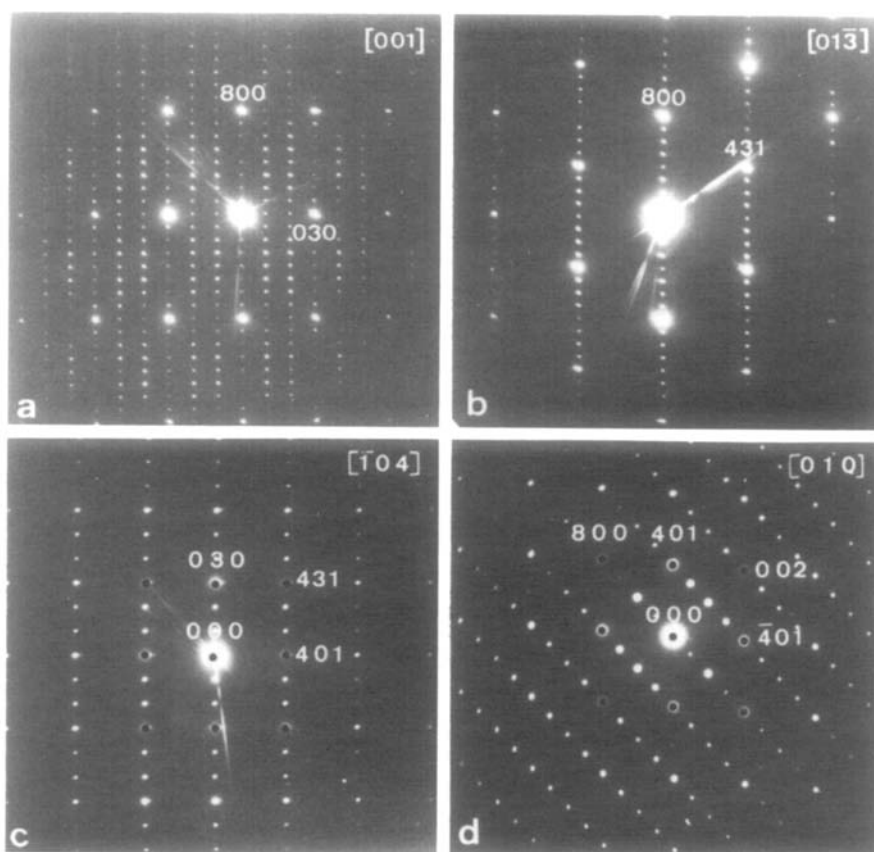


FIG. 2. Diffraction patterns of krennerite along different zones: (a)  $[001]$ , (b)  $[01\bar{3}]$ , (c)  $[\bar{1}04]$ , (d)  $[010]$ .

eightfold periodicity. Among the *hol* spots only those for which  $h = \text{even}$ , should be present; this is visible in Fig. 2d which represents the  $[010]$  zone. In this zone the distance from the origin to the 800 spot is therefore divided in only four parts by superstructure spots. The *hoo* spots should in fact be absent except for  $h = \text{eightfold}$ ; the presence of spots with  $h \neq 8n$  is due to double diffraction. The streaking through the central spot results from the use of a triangular selective diaphragm and has no further physical meaning. The superstructure spots of the type *hko* with  $k = \text{threefold}$ , are very weak; they are not prohibited by the space group. They are presumably

due at least in part to double diffraction. Figure 2c as well as Fig. 2d are pseudocubic sections, the cubic reflections being indicated by black dots.

The sections of reciprocal space reproduced in Fig. 2 are all consistent with the structure of Fig. 1. The sharpness of the spots suggests that the structure is rather perfect and presents little variability.

The pattern of Fig. 2a can be analysed in terms of repeat twinning using the method described in Ref. (4) and which makes use of the geometry of the pattern only. The model deduced in this manner can be noted as (4,4); which is in accordance with the structure as described in Ref. (1).

### 5. High Resolution Image

The most informative image is expected to be that taken along the  $[001]$  zone represented in Fig. 3 since it should clearly exhibit the twin structure. Figure 3 does in fact exhibit a "chevron" arrangement of bright dots. The configuration of these bright dots is the same, in scale and in orientation, as that of gold and silver columns in krennerite. The white zigzag line in Fig. 3 emphasizes the linear arrangements of bright dots, each line segment contains five dots corresponding with the five columns of heavy metal atoms connected by double lines in Fig. 1a.

Exceptionally one finds isolated wider strips of calaverite structure. In Fig. 4 two

such wide strips, indicated by arrows 1 and 2, are visible. They both have approximately double the normal width of the twin strips in the ideal krennerite structure. The strips 1 and 2 are also one relative to the other in a twin relationship.

Strip 2 is not constant in width; in one part it contains 11 rows of metal columns; in another part it contains 12 such rows; this clearly implies that also the adjacent strip changes in width. The twin interface thus contains a ledge.

A magnified image of strip 1 is reproduced in Fig. 5. The presence of strips of a different width suggests that possibly structures with different periods might occur. We have systematically looked for different twin interface modulated structures, as well

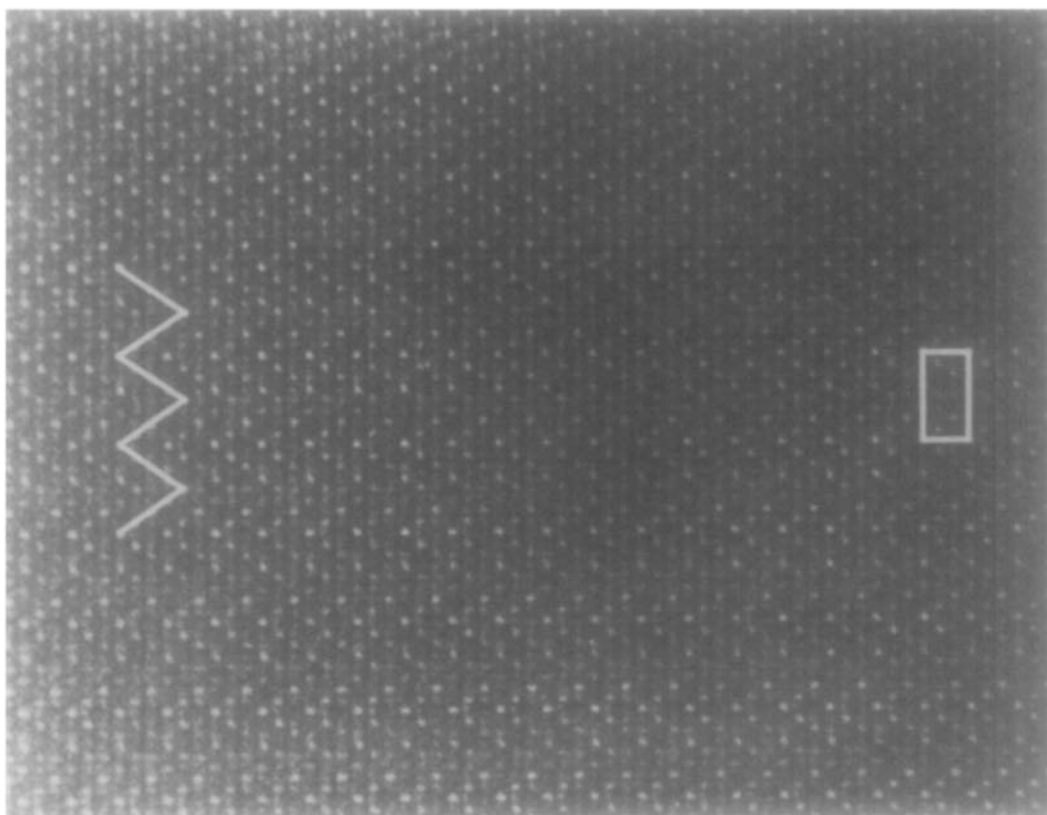


FIG. 3. High resolution image of krennerite taken along the  $[001]$  zone. Note the chevron arrangement of bright dots, emphasized by the white zigzag line. The projection of the unit cell is outlined.

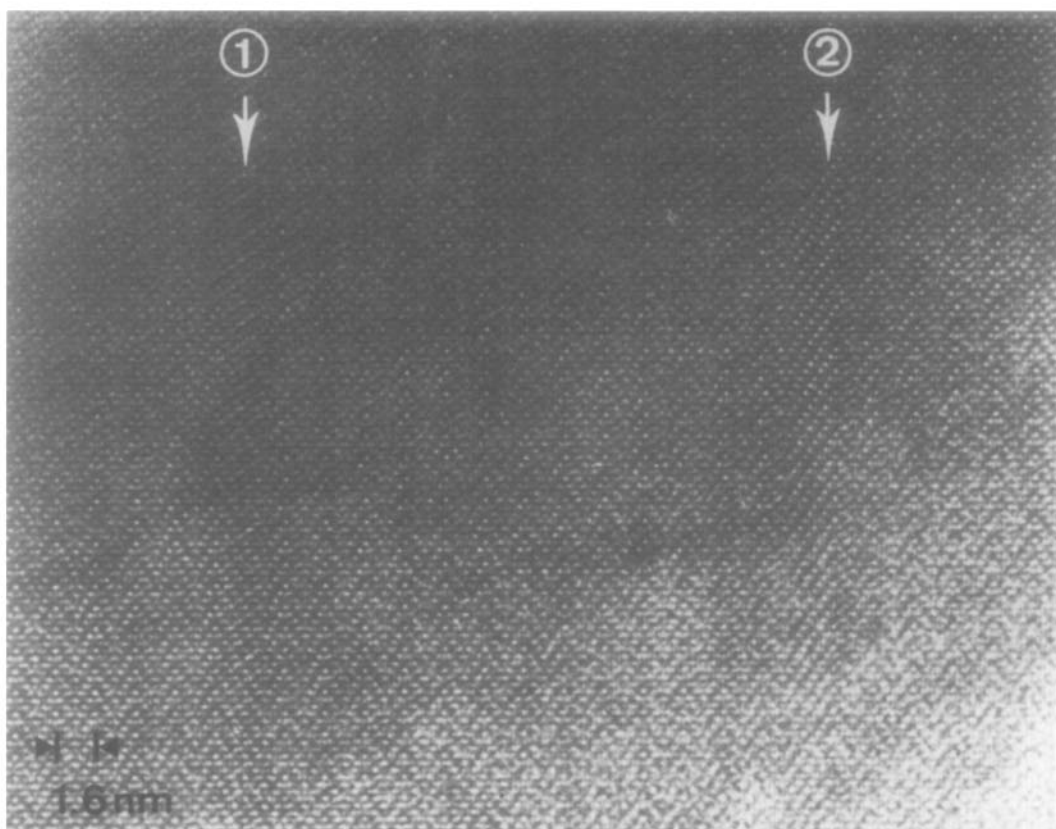


FIG. 4. High resolution image of krennerite containing two strips of a different width, marked 1 and 2. These two strips are twin related. Strip 2 is limited by a ledged twin interface.

in the diffraction pattern as in the high resolution images. So far we had no success in the composition range where krennerite is stable.

The pseudo hexagonal zone  $[01\bar{3}]$  is shown in Fig. 6. In the thinnest parts of the specimen a close-packed array of bright dots of uniform intensity reveals the basic structure. As the specimen becomes thicker the true period of about 1.6 nm becomes evident. It is quite a general feature that the long period of superstructures is best revealed in thick parts of the specimen, whereas the very thin parts only reveal the basic structures (in the present case, the primitive cubic lattice (5)).

Figure 7 reproduces an image along the

$[010]$  zone. The bright dots have the geometry and scale of the atom columns as seen along this zone. In the disordered structure of Fig. 1b all columns are chemically identical; they contain two tellurium atoms and one heavy metal atom in succession. Every fourth column row along the vertical direction in Fig. 7 is somewhat brighter. We shall show that this is presumably due to ordering of gold and silver in such a way that silver is situated along the twin plane.

## 6. Image Calculations

The image simulation method used in this study was already referred to previously in parts I and II. The same method was ap-

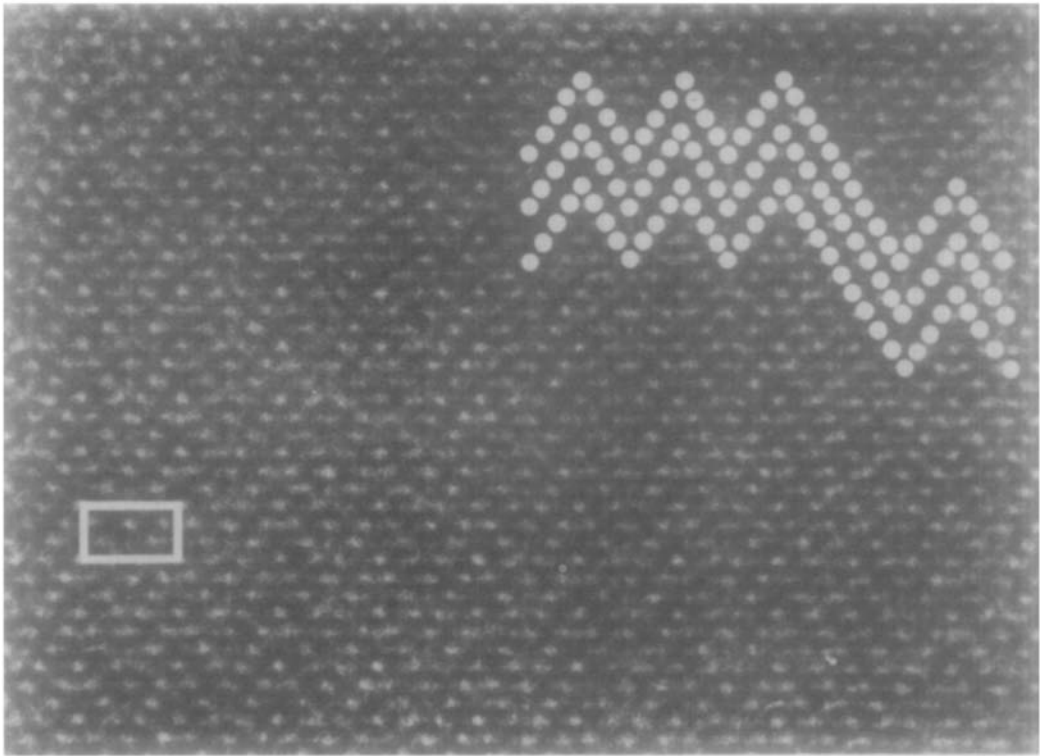


FIG. 5. Magnified image of wider strip. The projection of the unit cell is indicated. The bright dots mark heavy atom columns.

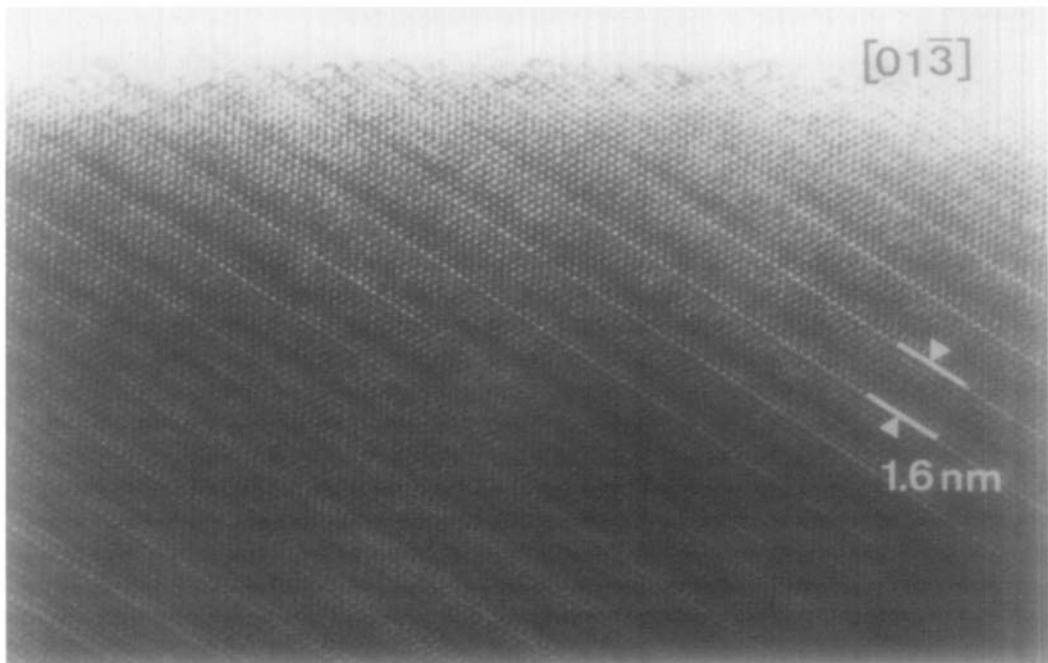


FIG. 6. High resolution image along the  $[01\bar{3}]$  zone. In the thinnest part of the wedge-shaped specimen only the pseudohexagonal basic structure is revealed; in the thicker part the superstructure is obvious.

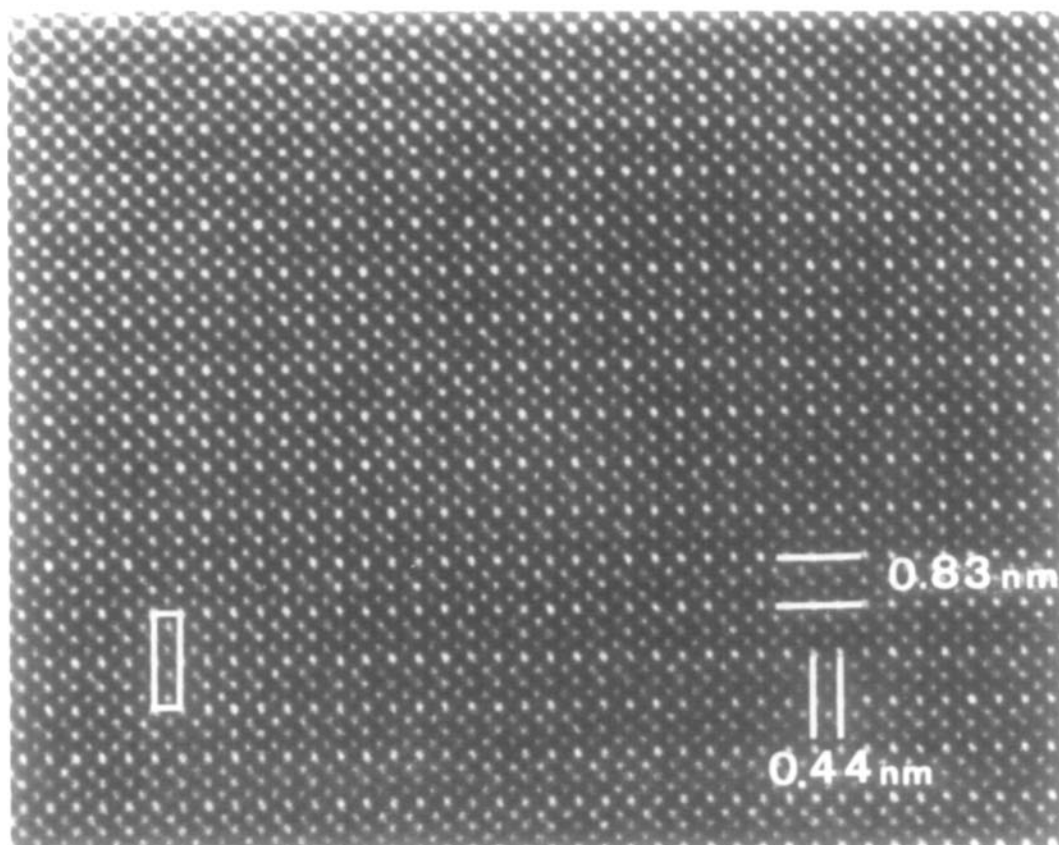


FIG. 7. High resolution image along the [010] zone. This image can be compared with Fig. 1b.

plied in the present case to compute images along the [001] and [010] zones, which are considered to be the most relevant ones.

In the [001] zone a matrix of images corresponding to foil thicknesses ranging from 5 to 20 nm and for defocus values  $\Delta f$  of  $-90$  and  $-96$  nm is reproduced in Fig. 8. These are the images which best reveal the chevron structure. However, the images are extremely sensitive to small variations of these two parameters. This was found to be the case experimentally as well. We have limited ourselves to images which are directly interpretable in terms of heavy metal columns. The best fit with the experimental images of Fig. 3, although not perfect, was obtained for  $t = 20$  nm and  $\Delta f = -96$  nm.

The chevron configuration, with the cor-

rect angle, can be recognized but the gold (or silver) columns are not as prominently represented as bright dots as is the case in the experimental images. We have computed images where all heavy atoms are the same as well as images with silver atoms in the columns along the twin interfaces and gold atoms elsewhere. No significant difference in fit between computed and experimental images was found in this zone.

We have also computed images as viewed along the [010] zone; again as well with gold as with silver along the twin interfaces and gold elsewhere. Computed images of the [010] zone, assuming silver along the twin interfaces, are reproduced in Fig. 9 for three different thicknesses and two defocus values. The fourfold periodic-

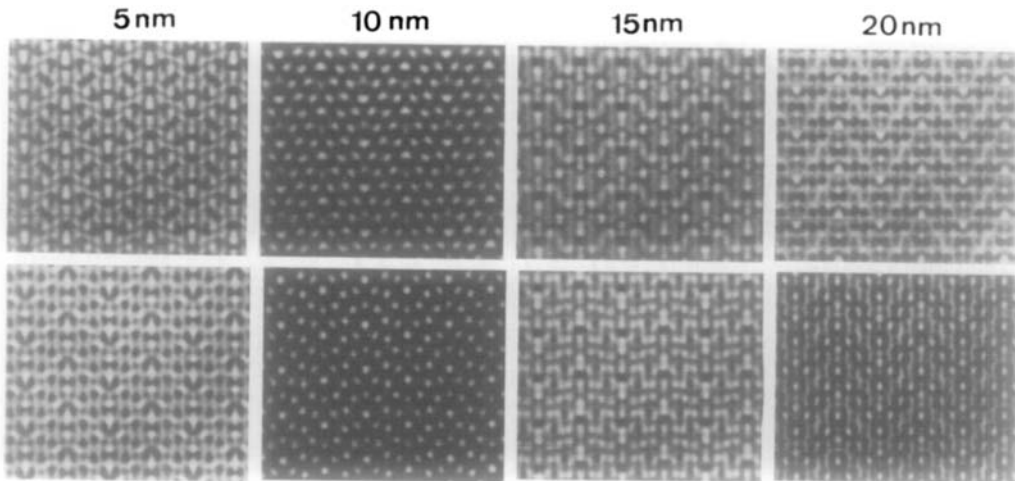


FIG. 8. Matrix of computer-simulated images along the [001] zone. The thickness values are from left to right 5–10–15–20 nm; the upper and lower row correspond with defocus values, respectively, of  $-90$  and  $-96$  nm. The computed image for  $t = 20$  nm and  $\Delta f = -96$  nm gives the best fit with the experimental image of Fig. 3.

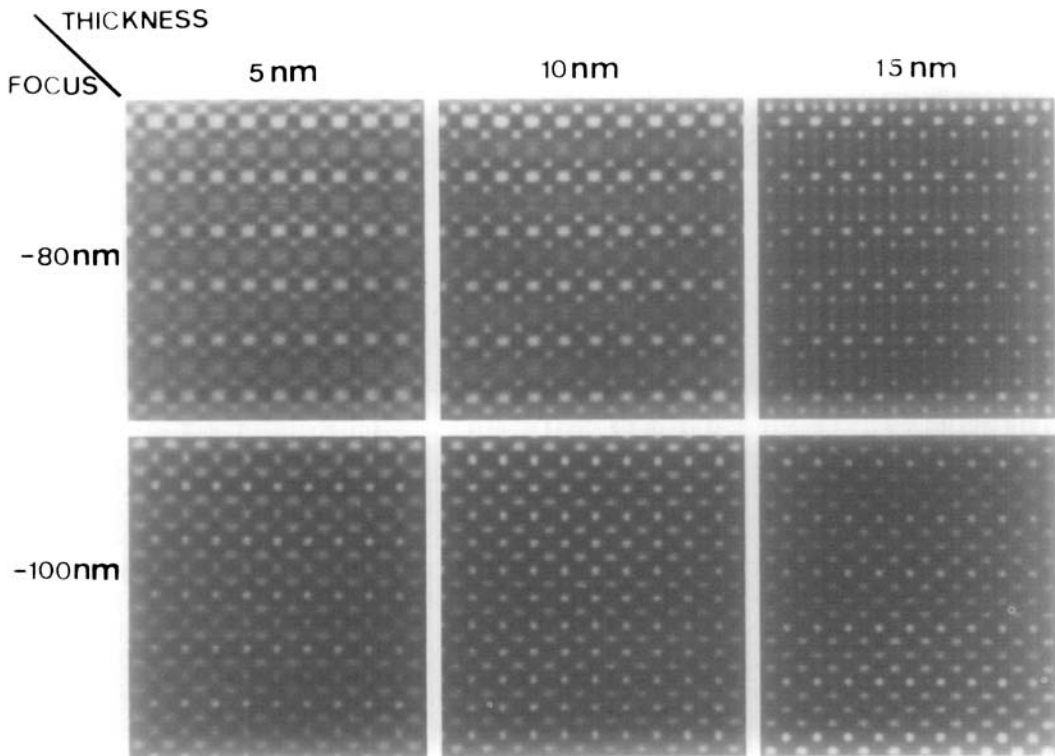


FIG. 9. Matrix of computer-simulated images along the [010] zone. The image with  $t = 15$  nm and  $\Delta f = -100$  nm gives the best fit with the experimental image.



ity, which appears in the experimental images at a sufficient thickness, is also apparent in some of the computed images. This was less pronounced in the case where all heavy atoms were considered to be the same. This seems to suggest that possibly the silver atoms are situated exclusively or at least preferentially along the twin interfaces.

## 7. Discussion

By the combination of electron diffraction and electron microscopy it has been possible to confirm unambiguously the structure of krennerite as proposed by Tunell and Pauling (3). Moreover our observations shed some light on the question whether or not gold and silver are ordered in krennerite. This problem remained unsettled in Ref. (3).

It was already established that gold and silver atoms order in sylvanite (2, 3). It is therefore not unreasonable to expect that they would do the same in krennerite. If the silver atoms should adopt an ordered arrangement which changes neither the unit cell nor the space group, this might well go unnoticed in an X-ray diffraction experiment. These conditions would be satisfied if silver atoms are assumed to occupy sites along the twin interfaces. This assumption would moreover lead to a chemical composition which is compatible with the composition range within which krennerite is known to occur. If every twin site would be occupied by silver and the other heavy metal sites by gold the composition would be  $\text{Ag}_{0.25}\text{Au}_{0.75}\text{Te}_2$ .

The observed images seem to support such an assumption.

Conversely one might speculate that the silver atoms may play a role in inducing twinning because silver atoms prefer to be

surrounded by tellurium in a different manner than do gold atoms (3).

We tried to vary the composition in the neighborhood of the ideal krennerite composition hoping to induce in this way different spacings between twin planes. This was unsuccessful because under these conditions we obtained two-phase materials containing also calaverite or sylvanite. Occasionally twin lamella of a different width occurred, but not in regular arrays. The range of compositions within which the krennerite phase exists seems to be rather narrow. Moreover other factors than merely the composition apparently determine the period of the polysynthetic twins.

Remarkably enough of the modulation wavelength, observed in the whole composition interval between calaverite ( $\text{AuTe}_2$ ) and sylvanite ( $\text{Au}_{0.5}\text{Ag}_{0.5}\text{Te}_2$ ), is always in the same range, i.e., equal to  $4-4.5 d_{202}$ . The modulation mechanisms are different however. Whereas calaverite is deformation modulated (1), sylvanite is antiphase boundary modulated (2), and finally krennerite is twin modulated. In the latter case the distance between twin interfaces is  $4d_{202}$  but the crystallographic period is  $8d_{202}$ .

## References

1. G. VAN TENDELOO, P. GREGORIADES, AND S. AMELINCKX, *J. Solid State Chem.* **50**, 321 (1983).
2. G. VAN TENDELOO, P. GREGORIADES, AND S. AMELINCKX, *J. Solid State Chem.* **50**, 335 (1983).
3. G. TUNELL AND L. PAULING, *Acta Crystallogr.* **5**, 375 (1952).
4. D. VAN DYCK, D. COLAITIS, AND S. AMELINCKX, *Phys. Status Solidi (A)* **68**, 419 (1981); "Proceedings, 10th International Congress on Electron Microscopy, Hamburg," Vol. 2, p. 117. Deutsche Gesellschaft für Elektronenmikroskopie, Frankfurt, 1982.
5. D. VAN DYCK, G. VAN TENDELOO, AND S. AMELINCKX, *Ultramicroscopy* **10**, 263 (1982).